High-frequency spin waves in $YBa_2Cu_3O_{6.15}$

S. M. Hayden
H. H. Wills Physics Laboratory, University of Bristol, Tyndall Avenue, Bristol BS8 1TL, United Kingdom

G. Aeppli*
AT&T Bell Laboratories, Murray Hill, New Jersey 07974

T. G. Perring
ISIS Facility, Rutherford Appleton Laboratory, Chilton, Didcot, OX11 0QX United Kingdom

H. A. Mook
Oak Ridge National Laboratory, Oak Ridge, Tennessee 37831

F. Doğan
Department of Materials Science and Engineering, University of Washington, Seattle, Washington 98195
(Received 20 June 1996)

Pulsed neutron spectroscopy is used to absolute measurements of the dynamic magnetic susceptibility of insulating $YBa_2Cu_3O_{6.15}$. Acoustic and optical modes, derived from in- and out-of-phase oscillation of spins in adjacent CuO_2 planes, dominate the spectra and are observed up to 250 meV. The optical modes appear first at 74 ± 5 meV. Linear-spin-wave theory gives an excellent description of the data and yields intralayer and interlayer exchange constants of $J_{\|}=125\pm5$ meV and $J_{\perp}=11\pm2$ meV, respectively, and a spin-wave intensity renormalization $Z_{\chi}=0.4\pm0.1$. [S0163-1829(96)52734-7]

The fundamental building blocks of the high-T_c superconductors are (nearly) square lattices of Cu atoms linked to their nearest Cu neighbors via the p orbitals of intervening oxygen atoms. The blocks occur in units of one, two, or three layers, which, in turn, are separated from each other by spacers serving as charge reservoirs. In general, the superconducting transition temperature rises with the number of CuO_2 layers in the units. This means that multilayer materials, most notably $YBa_2Cu_3O_{6+x}$ ($T_c=93$ K), have received much more attention than single-layer materials such as $La_{2-x}Sr_xCuO_4$ ($T_c=38$ K). Even so, the magnetic fluctuations, which are popular as a potential source of high-T_c superconductivity, have been characterized over a much wider range of frequencies (ω) and momenta ($\mathbf{Q}$) for $La_{2-x}Sr_xCuO_4$ (Refs. 1–5) than for $YBa_2Cu_3O_{6+x}$.[6–9] Indeed, while $La_{2-x}Sr_xCuO_4$, for both insulating and superconducting compositions, has been studied throughout the Brillouin zone for $\hbar\omega$ up to 0.4 eV, magnetic excitations in $YBa_2Cu_3O_{6+x}$ have only been observed for $\hbar\omega$ comparable to, or below, the pairing energy (40 meV) and thus much less than the likely coupling $J_{\|}$ responsible for the antiferromagnetism of the insulating parent. We have consequently performed magnetic neutron-scattering experiments to establish the spin dynamics of $YBa_2Cu_3O_{6+x}$ on a high-energy scale. The sample chosen for this first measurement is an insulating antiferromagnet with $x=0.15$. Our study reveals spin-wave excitations up to 0.25 eV. Below $\hbar\omega_g=74\pm5$ meV, we observe only acoustic spin waves where pairs of neighboring spins in adjacent planes rotate in the same sense about their average direction. Above $\hbar\omega_g$, we have discovered optical spin waves,[10] where the spins in adjacent planes rotate in opposite directions, thus sensing the restoring force from the interplanar coupling $J_{\perp}$. Our data are well described by a linear spin-wave model in which an overall quantum renormalization of the spin-wave intensity $Z_{\chi}=0.4\pm0.1$ ($Z_{\chi}=1$ for the classical limit) is included and the intraplanar and interplanar exchange constants are $J_{\|}=125\pm5$ meV and $J_{\perp}=11\pm2$ meV respectively.

Experiments were performed on the high energy transfer (HET) spectrometer at the ISIS pulsed spallation source of the Rutherford-Appleton Laboratory. The experimental techniques for measuring high-frequency spin fluctuations using a direct-geometry chopper spectrometer such as HET are described elsewhere.[3] The sample used in the present investigation was a single crystal of $YBa_2Cu_3O_{6.15}$ with mass 96 g. The oxygen composition was determined gravimetrically and room-temperature lattice constants were $a=b=3.857$ Å and $c=11.84$ Å corresponding to a Néel temperature of 400 K.[6] In common with other large single crystals of $YBa_2Cu_3O_{6+x}$, our sample contains Y_2BaCuO_5 as an impurity phase. This was determined to constitute 12% of the mass by neutron diffraction from a substantial powdered piece of our sample. We index reciprocal space using the tetragonal unit cell so that antiferromagnetic Bragg peaks occur at $(\frac{1}{2},\frac{1}{2},0)$ and related positions, momentum transfers (Q_x,Q_y,Q_z) in units of Å^{-1} are then at reciprocal space positions $(h,k,l)=(Q_xa/2\pi,Q_yb/2\pi,Q_zc/2\pi)$. Measurements were made with the $(1\bar{1}0)$ plane coincident with the horizontal scattering plane of the spectrometer. The detectors are 300-mm-long 25-mm-diameter tubes at 2.5 or 4 m from the sample with scattering angles in the range $2.5°<2\theta<28°$. Absolute unit conversions were performed by measuring the elastic incoherent scattering from a vana-

dium standard under the same experimental conditions.[5] Data were collected at ambient temperature ($T=296$ K).

For the purpose of this experiment, we model $YBa_2Cu_3O_{6+x}$ as a set of weakly coupled CuO_2 biplanes, i.e., a square-lattice bilayer antiferromagnet. We neglect smaller interaction terms, such as the local anisotropy, which have little effect on the high-frequency excitations. In this case, the high-frequency spin dynamics can be described using the Heisenberg Hamiltonian for a single bilayer

$$H=\sum_{ij} J_{\parallel}\mathbf{S}_i\cdot\mathbf{S}_j+\sum_{ij'} J_{\perp}\mathbf{S}_i\cdot\mathbf{S}_{j'}, \tag{1}$$

where the first term represents the nearest-neighbor coupling between Cu-II spins in the same plane and the second the nearest-neighbor coupling between Cu spins in different planes. The introduction of the second term in Eq. (1) leads to two branches in the spin-wave dispersion[6] which are labelled according to whether nearest-neighbor spins in different planes rotate together (acoustic mode) or in opposite directions (optical mode) about their average directions. Conventional linear-spin-wave theory of the Holstein-Primakoff type yields the imaginary part of the dynamic susceptibility (per formula unit) for the two modes as:

$$\chi''_{\mathrm{op}}(Q,\omega)=\frac{\pi g^2\mu_B^2}{\hbar}S\left(\frac{1-\gamma(Q)}{1+\gamma(Q)+J_{\perp}/2J_{\parallel}}\right)^{1/2}\times\cos^2\left(\frac{1}{2}\Delta z Q_z\right)\delta[\omega\pm\omega_{\mathrm{op}}(Q)] \tag{2}$$

and

$$\chi''_{\mathrm{ac}}(Q,\omega)=\frac{\pi g^2\mu_B^2}{\hbar}S\left(\frac{1-\gamma(Q)+J_{\perp}/2J_{\parallel}}{1+\gamma(Q)}\right)^{1/2}\times\sin^2\left(\frac{1}{2}\Delta z Q_z\right)\delta[\omega\pm\omega_{\mathrm{ac}}(Q)], \tag{3}$$

where the dispersion relations are

$$\hbar\omega(Q)=2J_{\parallel}\{1-\gamma^2(Q)+J_{\perp}/2J_{\parallel}[1\pm\gamma(Q)]\}^{1/2} \tag{4}$$

(the plus sign is for the acoustic mode), $\gamma(Q)=1/2[\cos(aQ_x)+\cos(aQ_y)]$ and $\Delta z(=3.2$ Å) is the separation of the CuO_2 bilayers. With the coupling terms in Eq. (1), there is no dispersion along the z direction, only a modulation of the amplitude of the dynamic susceptibility, which may be used to distinguish the two modes. Further, the energy of the optical branch shows a minimum at $\mathbf{Q}=(\frac{1}{2},\frac{1}{2},l)$ of $\hbar\omega_g=2\sqrt{J_{\parallel}J_{\perp}}$.

By varying the incident neutron energy E_i, we can arrange to cut across the spin waves at given energy transfers $\hbar\omega$ and values of $Q_z(l)$. Figures 1(b)–1(e) show data collected as a function of $\mathbf{Q}$ parallel to the (110) direction for various energy transfers $\hbar\omega$ such that $\sin^2(\frac{1}{2}\Delta z Q_z)\approx 1$, i.e., $l=Q_z c/2\pi=1\times 8,5\times 5,\ldots$. Under these conditions, we are sensitive only to modes with acoustic character. At all frequencies, we observe a peak near $\mathbf{Q}=(\frac{1}{2},\frac{1}{2},l)$ corresponding to the spin waves. Twin peaks, due to counter-propagating spin-wave branches, are not seen due to the poor out-of-plane resolution (see Fig. caption) in the (110) direction. Figures 1(g)–1(j) show similar data collected such that

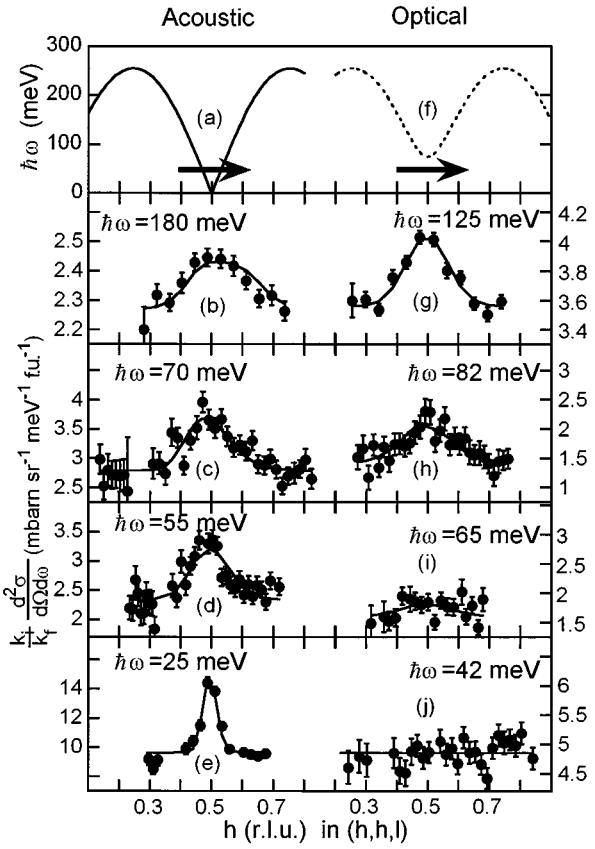

FIG. 1. (a) and (f) show the dispersion relations for acoustic and optical spin-wave branches respectively. Remaining panels are energy scans showing magnetic scattering from $YBa_2Cu_3O_{6.15}$ for wave-vector transfers $\mathbf{Q}=(h,h,l)$. (b)–(e) l is chosen to give scattering from acoustic modes. (g)–(j) l is chosen to give scattering from optical modes. Incident energies and Q_z wave-vector components are $E_i=600$, 110, 75, 75, 600, 110, 75, 75 meV and $l=5.3$, 5.5, 1.9, 3.6, 7.2, 7.1, 3.7 for (b)–(e), (g)–(j) respectively. For the instrumental configuration used for panel (c) and Fig. 3, the resolution in energy was 2 meV and in Q was 0.05 Å^{-1} in the scattering plane and 0.5 Å^{-1} perpendicular to it (all widths quoted as full width at half maximum).

$\cos^2(\frac{1}{2}\Delta z Q_z)\approx 1$, i.e., $l=3.7,7.3,\ldots$. In this case, we are sensitive only to optical modes. Little or no magnetic scattering is evident below 82 meV. (The area under the 65 meV peak is approximately 10 times smaller than for 82 meV.) Our observations are in agreement with thermal neutron-scattering studies,[6–8] made with $\hbar\omega\leqslant 42$ meV, which showed a $\sin^2(\frac{1}{2}\Delta z Q_z)$ modulation of the magnetic scattering at low-energy transfers. In order to make a more quantitative interpretation we use our data to calculate the two-dimensional (2D) local- or wave-vector-integrated susceptibility $\chi''_{2\mathrm{D}}(Q_z,\omega)=\int\chi''(Q,\omega)d^2Q/\int d^2Q$, where the $\mathbf{Q}$ integrals are over (Q_x,Q_y) only and Q_z is chosen to be close to an optical or acoustic position. The poor out-of-plane resolution means that the integration of the spin-wave signal over components of momentum transfer perpendicular to the scattering plane is carried out automatically. The results are shown in Fig. 2. When the data are plotted in this way, it is clear that for energies $\hbar\omega\geqslant 82$ meV, the optical and acoustic intensities are equal within experimental error. On the other

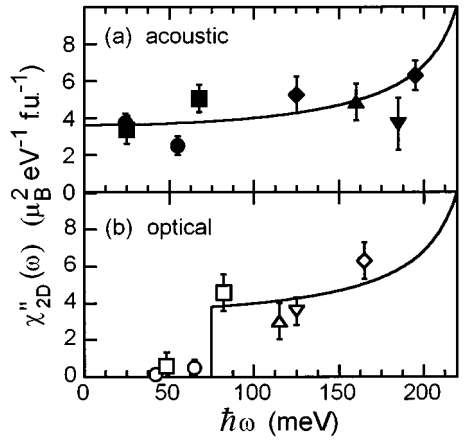

FIG. 2. The 2D local susceptibility as a function of energy transfer obtained by integrating over spin-wave peaks and correcting for the Cu^{2+} magnetic form factor, Bose factor, and instrumental resolution. (a) acoustic positions and (b) optical positions. The figure is a compilation based on the analysis of data such as those in Fig. 1 with various incident energies. Solid lines correspond to fits to spin wave theory.

hand, for $\hbar\omega \leqslant 65$ meV, the integrated response at the optical position is consistent with zero. Thus $\hbar\omega_g$ lies between 65 and 82 meV.

A more accurate estimate of the optical gap can be made from Fig. 3. This spectrum shows data collected as a function of $\hbar\omega$ with $E_i = 110$ meV and integrated over wave vectors with $0.45 \leqslant h \leqslant 0.55$, i.e., over the spin-wave cones emanating from $(\frac{1}{2},\frac{1}{2},l)$. The integration range is restricted to reduce phonon contamination in the spectrum. Due to energy and momentum conservation in the scattering process, Q_z varies with $\hbar\omega$ in the way indicated by the horizontal axes of Fig. 3. Thus, Fig. 3 displays the local susceptibilities associated with the acoustic and optical modes, weighted by their

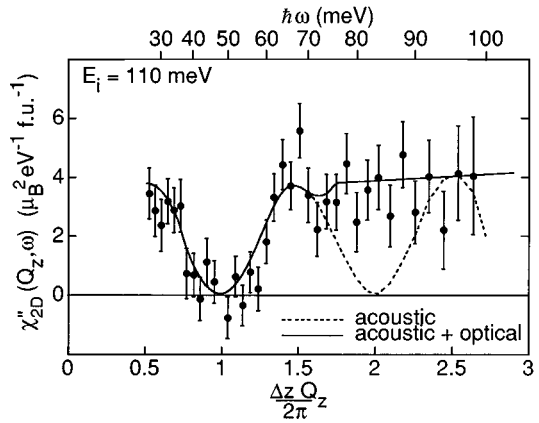

FIG. 3. Data collected with $E_i = 110$ meV, integrated over the spin-wave cones in the (Q_x,Q_y) plane near $Q=(\frac{1}{2},\frac{1}{2},l)$ and corrected for the Cu^{2+} magnetic form factor and Bose factor. The resulting spectrum is collected along a trajectory in $(Q_z,\hbar\omega)$ defined on the upper and lower axes. Under these conditions the sinusoidal intensity modulation with Q_z will disappear at $\hbar\omega_g \approx 74$ meV. Solid line corresponds to a fit to spin wave theory. Dotted line is the acoustic mode contribution.

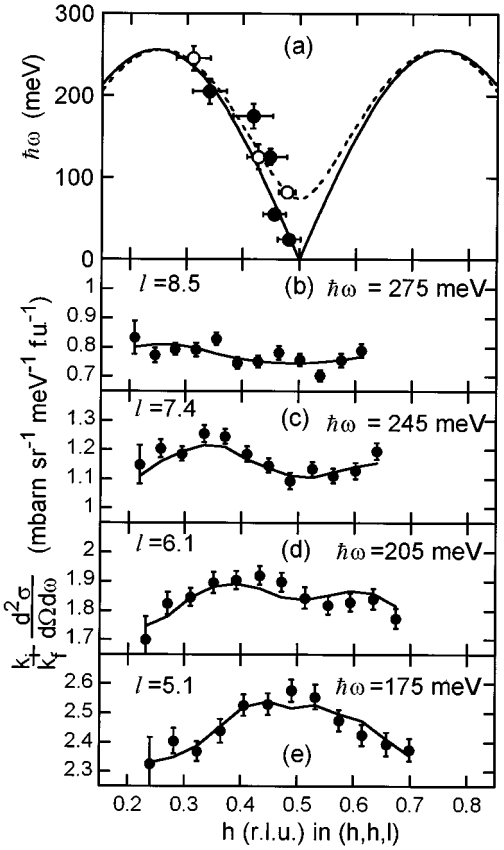

FIG. 4. (a) The dispersion relation obtained from independent fits at each energy transfer (all data in paper). Closed circles and solid line are for acoustic modes, open circles and dotted line are optical modes. (b)–(e) Constant energy scans showing high-frequency magnetic scattering from $YBa_2Cu_3O_{6.15}$. Data were collected with $\mathbf{k}_i \| (001)$ and $E_i = 600$ meV. Counting time was 29 h at 170 μA proton current with a Ta target. Solid lines are resolution-corrected fits of a linear spin-wave model for a bilayer (see text). Resolution widths were $\Delta\hbar\omega = 20$ meV and $\Delta Q = 0.1$ and 1 Å^{-1} parallel and perpendicular to the scattering plane, respectively.

Q_z-dependent structure factors. At lower frequencies ($\hbar\omega \lesssim J_\parallel$), the 2D local susceptibility associated with the acoustic mode is essentially ω independent and that associated with the optical mode has a step at $\hbar\omega_g$ (see solid lines in Fig. 2). Consequently, in Fig. 3 we expect to observe a simple sinusoidal modulation with Q_z due to the acoustic mode, $\chi''_{2D}(Q_z,\omega) \propto \sin^2(\frac{1}{2}\Delta z Q_z)$ for $\omega < \omega_g$. For $\omega \geqslant \omega_g$, a second sinusoidal modulation of almost equal amplitude and $\pi/2$ out of phase, due to the optical mode, is superposed, yielding a Q_z- (and ω-) independent signal. By inspection, we can see that above approximately 70 meV the intensity is constant and below this value the characteristic acoustic modulation is observed. A resolution-corrected fit of Eqs. (2)–(4) to the data yields a value[10] for the optical gap of $\hbar\omega_g = 74 \pm 5$ meV.

The optical mode gap is simply proportional to the geometric mean of $J_\parallel$ and $J_\perp$, and so by itself, its measurement establishes neither $J_\perp$ nor $J_\parallel$. Indeed, to determine $J_\parallel$ and $J_\perp$, it is necessary to determine not only $\hbar\omega_g$, but also the spin-wave dispersion as a function of in-plane momentum. We have therefore collected data at energy transfers sufficiently large to make the dispersion obvious. Figure 4 shows

the results obtained for an incident energy $E_i = 600$ meV. For $\hbar\omega = 175 \pm 15$ meV, the scattering, though broadened by the dispersion, is still peaked at $(\frac{1}{2}, \frac{1}{2}, l)$. For $\hbar\omega = 245 \pm 15$ meV, the dispersion causes the scattering to be peaked near $(0.35, 0.35, l)$. Finally, for slightly larger energy transfer $\hbar\omega = 275 \pm 15$ meV, there is a much diminished modulation, consistent with a cutoff of approximately 250 meV for single-magnon scattering. The solid lines in Figs. 4(b)–4(e) show resolution-corrected fits of linear spin-wave theory. From fitting each energy individually, we determine the dispersion relations shown in Fig. 4(a). A simultaneous fit including the lower frequency data (see solid lines in Figs. 1–3 yields exchange constants $J_\parallel = 125 \pm 5$ meV and $J_\perp = 11 \pm 2$ meV.

A range of values for $J_\parallel$ have been inferred from other measurements. Rossat-Mignod and coworkers[7] deconvolved reactor-based measurements of low-frequency spin waves and found a spin-wave velocity, near $(\frac{1}{2}, \frac{1}{2}, l)$, of $\hbar c = 1000 \pm 50$ meV Å , which if we assume the absence of further neighbor interactions (confirmed by the present experiment), implies $J_\parallel \approx 200$ meV. Shamoto *et al.*[8] performed a similar study and found $\hbar c = 655 \pm 100$ meV Å . This is in agreement with the initial slope of the acoustic dispersion curve we have measured. The only preexisting information on the magnetic energy scale at short wavelengths is from interpretation of the two-magnon Raman effect,[11] which suggests, for a model including only a single near-neighbor exchange, $J_\parallel \approx 120$ meV. Our value for $J_\parallel$ is substantially below that (0.16 eV) (Ref. 3) for La_2CuO_4. This discrepancy may be due to greater off stoichiometry in our $YBa_2Cu_3O_{6.15}$ sample as well as its larger lattice constants.

It is well known that in two-dimensional quantum antiferromagnets, the spin-wave energies and the overall intensity of the spin waves show quantum renormalizations Z_c and Z_χ respectively[12,13] when compared with their classical (large S) values. Neutron scattering cannot directly measure Z_c, thus the bare exchange constants must be inferred from our effective or measured coupling constants using theoretical estimates[12] of $Z_c \approx 1.18$. In contrast, we are able to measure Z_χ experimentally by placing our measurements on an absolute intensity scale. Following this procedure, we obtain a value of $Z_\chi = 0.4 \pm 0.1$, close to that ($Z_\chi = 0.51$) given by a $1/S$ spin-wave expansion[13] and indistinguishable from that given by our measurements[5] on La_2CuO_4.

Not as much is known about $J_\perp$ as about $J_\parallel$ and Z_χ. Even so, detailed analysis[14] of the essentially zero-frequency magnetic response measured[15] by nuclear resonance for $Y_2Ba_4Cu_7O_{15}$ suggests $5 < J_\perp < 20$ meV. It is also interesting to ask what happens to $J_\perp$ in the metallic and superconducting samples, especially because one explanation[16] for the celebrated spin gap behavior of $YBa_2Cu_3O_{6+x}$, which is not so clearly seen in the single layer compounds, requires $J_\perp \neq 0$. Magnetic scattering for all superconducting samples of $YBa_2Cu_3O_{6+x}$ displays the modulation characteristic of acoustic spin-wave modes.[7,9] Because scattering has been observed up to $\hbar\omega \approx 45$ meV $= 0.6\hbar\omega_g (x = 0.15)$, the bilayer coupling for even the optimally doped superconductor is unlikely to be much smaller than 4 meV or 45 K which is 36% $(= 0.6^2)$ of $J_\perp (x = 0.15)$.

In summary, we have measured single-magnon excitations in the insulating antiferromagnet $YBa_2Cu_3O_{6.15}$ throughout the Brillouin zone. Our results are well described by a linear spin-wave model for a 2D square bilayer, provided an appropriate overall amplitude renormalization is included. The resulting interplanar and intraplanar exchange constants are $J_\parallel = 125 \pm 5$ meV and $J_\perp = 11 \pm 2$ meV respectively.

The support of the UK-EPSRC and the US-DOE at Bristol, ISIS, and Oak Ridge is gratefully acknowledged.

*Present address: NEC Research Institute, 4 Independence Way, Princeton, NJ 08540.

[1] D. Vaknin *et al.*, Phys. Rev. Lett. **58**, 2802 (1987); G. Shirane *et al.*, *ibid.* **59**, 1613 (1987).
[2] G. Aeppli *et al.*, Phys. Rev. Lett. **62**, 2052 (1989).
[3] S. M. Hayden *et al.*, Phys. Rev. Lett. **67**, 3622 (1991).
[4] S. Itoh *et al.*, J. Phys. Soc. Jpn. **63**, 4542 (1994).
[5] S. M. Hayden *et al.*, Phys. Rev. Lett. **76**, 1344 (1996); C. G. Windsor, *Pulsed Neutron Scattering* (Taylor and Francis, London, 1981).
[6] J. M. Tranquada *et al.*, Phys. Rev. Lett. **60**, 156 (1988); Phys. Rev. B **40**, 4503 (1989).
[7] J. Rossat-Mignod *et al.*, J. Phys. (France) **49**, C8-2219 (1989); Physica B **169**, 58 (1991).
[8] S. Shamoto *et al.*, Phys. Rev. B **48**, 13 817 (1993).
[9] H. A. Mook *et al.*, Phys. Rev. Lett. **70**, 3490 (1993); H. F. Fong *et al.*, *ibid.* **75**, 316 (1995).
[10] S. M. Hayden *et al.*, Bull. Am. Phys. Soc. **41**, 400 (1996). The result for the optic mode gap in this announcement appears consistent with that reported subsequently by D. Reznik *et al.*, Phys. Rev. B **53**, R14 741 (1996).
[11] K. B. Lyons *et al.*, Phys. Rev. Lett. **60**, 1988 (1988); R. R. P. Singh *et al.*, *ibid.* **62**, 2736 (1989).
[12] R. R. P. Singh, Phys. Rev. B **39**, 9760 (1989).
[13] J. Igarashi, Phys. Rev. B **46**, 10 763 (1992).
[14] A. J. Millis and H. Monien (unpublished).
[15] R. Stern *et al.*, Phys. Rev. B **51**, 15 478 (1995).
[16] B. L. Altshuler and L. B. Ioffe, Solid State Commun. **82**, 253 (1992).